ARTICLE
Journal of Cellular Biochemistry 107:1160–1167 (2009)

Journal of Cellular Biochemistry

Modulation of Nucleocytoplasmic Trafficking by Retention in Cytoplasm or Nucleus

Daniela M. Roth,[1,2] Ian Harper,[3] Colin W. Pouton,[2] and David A. Jans[1*]

[1]*Nuclear Signalling Laboratory, Department of Biochemistry and Molecular Biology, Monash University, Monash, Vic. 3800, Australia*

[2]*Department of Pharmaceutical Biology, Victorian College of Pharmacy, Monash University, Parkville, Vic. 3052, Australia*

[3]*Monash Micro Imaging, Monash University, Monash, Vic. 3800, Australia*

ABSTRACT

Nuclear protein transport processes have largely been studied using in vitro semi-intact cell systems where high concentrations of nuclear localizing substrates are used, and cytoplasmic components such as the microtubule (MT) network, are either absent or damaged. Here we use the fluorescence recovery after photobleaching (FRAP) technique to analyze the nucleocytoplasmic flux of distinct fluorescently tagged proteins over time in living cultured cells. FRAP was performed in different parts of the cell to analyze the kinetics of nucleocytoplasmic trafficking and intranuclear/cytoplasmic mobility of the tumor suppressor Rb protein and a SV40 large tumor antigen (T-ag) derivative containing the nuclear localization sequence (NLS), both fused to green fluorescent protein (GFP). The results indicate that proteins carrying the T-ag NLS are highly mobile in the nucleus and cytoplasm. Rb, in contrast, is largely immobile in both cellular compartments, with similar nuclear import and export kinetics. Rb nuclear export was CRM-1-mediated, with its reduced mobility in the cytoplasm in part due to association with MTs. Overall our results show that nuclear and cytoplasm retention modulates the rates of nuclear protein import and export in intact cells. J. Cell. Biochem. 107: 1160–1167, 2009. © 2009 Wiley-Liss, Inc.

KEY WORDS: NUCLEAR IMPORT; NUCLEAR EXPORT; FRAP; RETINOBLASTOMA PROTEIN; SV40 LARGE TUMOR ANTIGEN

Protein transport between the nucleus and cytoplasm is limited by the nuclear envelope (NE) embedded nuclear pore complex (NPC), through which most transport is dependent on modular nuclear localization sequences (NLSs) [Gorlich and Kutay, 1999; Jans et al., 2000; Chan and Jans, 2002] and nuclear export sequences (NESs) [Fornerod et al., 1997], conferring transport in the import and export directions, respectively. Nuclear protein import/export relies upon the recognition of NLSs/NESs by members of the importin (IMP) superfamily of proteins, which mediate transport across the NPC. Most commonly, basic NLSs are recognized by either the IMPα/β heterodimer or IMPβ alone, whereas hydrophobic NESs rely on exportins such as CRM1 (exportin 1) for nuclear export [Henderson and Percipalle, 1997; Hubner et al., 1997; Forwood and Jans, 2002].

In vitro techniques relying on analysis of exogenously expressed/purified protein and cytoplasmic factors have been largely used to characterize the different NLS-dependent nuclear import pathways, and determine basic parameters of nuclear import kinetics [Jans and Jans, 1994; Seydel and Jans, 1996; Hu et al., 2005]. However, these methods are restricted to semi-intact or damaged cell systems that use high concentrations of nuclear localizing substrates and IMPs. In addition, the MT network, which has been implicated in facilitating the nuclear import of several proteins [Giannakakou et al., 2000; Lam et al., 2002; Roth et al., 2007], is either lacking or damaged in semi-intact cells, thus being completely disregarded in such approaches.

Here we use FRAP to analyze and compare the kinetics of nucleocytoplasmic trafficking, and mobility of two distinct NLS/NES containing proteins in living cells, including the tumor suppressor Rb full-length protein, and a small region of T-ag (including the NLS, but lacking all sequences responsible for conferring binding to DNA, Rb, p53 or Hsc/HSP70), as GFP-fusion proteins. The results indicate that proteins carrying the T-ag NLS are highly mobile in the nucleus and cytoplasm. Rb, in contrast, is largely immobile in both cellular compartments, with similar

Additional Supporting Information may be found in the online version of this article.

Grant sponsor: National Health and Medical Research Council; Grant number: 384107.

*Correspondence to: Prof. David A. Jans, Department of Biochemistry and Molecular Biology, Box 13D, Monash University, Vic. 3800, Australia. E-mail: david.jans@med.monash.edu.au

Received 10 November 2008; Accepted 22 April 2009 • DOI 10.1002/jcb.22218 • © 2009 Wiley-Liss, Inc.
Published online 8 June 2009 in Wiley InterScience (www.interscience.wiley.com).

nuclear import and export kinetics. Rb nuclear export is CRM-1-mediated as cells treated with the CRM-1 inhibitor, leptomycin-B (LMB), show a significantly slower rate of Rb nuclear export, with its reduced cytoplasmic mobility partially due to its association with MTs. Overall, the results show that cytoplasmic and nuclear retention strongly influence the rates of protein trafficking in intact cells.

MATERIALS AND METHODS

EXPRESSION CONSTRUCTS

Coding sequences were fused in frame C-terminal to that of GFP, using the Gateway™ compatible pEPI-DESTC plasmid [Ghildyal et al., 2005] for T-ag (amino acids 110–135, including the NLS and flanking protein kinase CK2 phosphorylation site) or pEGFP-C1 (Clontech) for Rb full-length (amino acids 1–928) [Markiewicz et al., 2002].

CELL CULTURE, TRANSFECTION, AND DRUG TREATMENTS

COS-7 cells were maintained in Dulbecco's modified Eagle's medium (DMEM), supplemented with 10% fetal calf serum (FCS) in a 5% CO_2 atmosphere at 37°C. Cells were transfected at 70–80% confluency using Lipofectamine 2000 (Invitrogen), according to the manufacturer's instructions, and imaged 20–24 h post-transfection. In some experiments, cells were treated for 4 h with 5 μg/ml nocodazole (NCZ, Sigma) prior to imaging to disrupt the MTs, as previously [Roth et al., 2007], or with 2.8 ng/ml LMB for 5–6 h to inhibit CRM-1-mediated nuclear export.

FRAP AND IMAGE ANALYSIS

FRAP was performed in COS-7 cells expressing the different GFP fusion proteins, using an Olympus Fluoview 1000 microscope equipped with an Argon ion laser (40 mW), and 100× oil immersion lens (Nikon) in combination with a heated stage. The photobleaching parameters were optimized according to the distinct cell compartment to be bleached, changing laser power, time of exposure, and size of the bleached area. Prior to bleaching, three images were collected using 3% of total laser power with excitation at 488 nm, scanning an area of 126 μm^2 at a rate of 8 μs/pixel. Nuclear bleaching was performed in an area covering approximately 4 μm^2 of the nucleus, scanning the area 10 times at a rate of 12.5 μs/pixel, and applying 80% of the laser power. For cytoplasmic bleaching, an area of c. 24 μm^2 was bleached, using 12 scans at a speed of 12.5 μs/pixel, and 100% laser power. After bleaching, the cells were immediately scanned and the recovery of fluorescence monitored by acquiring subsequent images at 20 s intervals for up to 10 min, using detector and laser settings identical to those prior photobleaching to minimize bleaching during post-bleach data collection. To visualize MT integrity after cytoplasmic bleaching, the cells were seeded in a gridded dish (Grid-500, Ibidi) 24 h before transfection. Transfection and bleaching of the cytoplasm was performed as above. Within 10–15 min after photobleaching the cells were rinsed with warm PBS, fixed with 4% paraformaldehyde/PBS for 25 min at room temperature, permeabilized with 0.1% Triton-X-100 in PBS/BSA 1% for 10 min, blocked with PBS/BSA 1% for 1 h, and incubated with anti-β-tubulin (1/500 dilution, Cytoskeleton) and Alexa™ 568-coupled secondary (1/1,000 dilution; Molecular Probes) antibodies for MT staining. After immunostaining bleached and non-bleached cells were compared by CLSM visualization for MT morphology.

Image analysis was carried out on the digitalized confocal files using the NIH public domain software Image J 1.38 as previously [Lam et al., 1999; Harley et al., 2003; Alvisi et al., 2005; Roth et al., 2007], to estimate the relative nuclear (Fn), cytoplasmic (Fc), and total cellular (FT) fluorescence above background fluorescence [Lam et al., 1999, 2002; Roth et al., 2007]. Results were expressed in terms of fractional recovery of Fn (FR_{Fn}) [Fn of respective time points (t_∞) divided by the prebleach Fn value] for nuclear bleaching, or of Fc for cytoplasmic bleaching (FR_{Fc}) [Fc of respective time points (t_∞) divided by the prebleach Fc value]. The fractional recovery values were then corrected for the loss of fluorescence during the bleaching and recovery period, using the equation: $F_{corrected} = FT_{prebleach}/FT_{t\infty} \times FR_{t\infty}$ [Phair and Misteli, 2000; Griffis et al., 2002]. For nuclear bleaching Fn/c ratios (fluorescence of the nucleus divided by the fluorescence of the cytoplasm above the background fluorescence) were also calculated for every time point during the bleaching, enabling determination of the extent of recovery in terms of Fn/c [Fn/c of respective time points (t_∞) divided by the prebleach Fn/c value] to remove the contribution of nucleocytoplasmic flux. Data was then fitted exponentially according to the formula $y = a(1 - e^{-bx})$ to determine the fractional recovery and the half time ($t_{1/2}$) values. Student's *t*-test or Mann–Whitney was carried out (see Table I) to determine the significance of the relative differences between different proteins or untreated and treated cells.

RESULTS

FRAP ANALYSIS OF NUCLEAR IMPORT SHOWS THAT RB IS HIGHLY IMMOBILE IN THE NUCLEUS

Nuclear photobleaching experiments were performed to compare the nuclear import and mobility of two distinct GFP-fusion proteins, the tumor suppressor Rb, and a sequence from T-ag (amino acids

TABLE I. FRAP Pooled Data for Fractional Recovery and Half Time ($t_{1/2}$)

GFP-	Recovery	*P*	$t_{1/2}$	*P*	n
Nuclear photobleach					
Rb	0.46 ± 0.04		70 ± 8		13
T-ag 110-135	0.89 ± 0.03	0.0001[a*,†]	41 ± 6	0.0157[a*,†]	12
Cytoplasmic photobleach					
Rb	0.41 ± 0.03		62 ± 5		17
Rb + LMB	0.40 ± 0.04	0.9577[a,†]	93 ± 10	0.0121[a*,†]	7
Rb + NCZ	0.51 ± 0.03	0.0463[a*,†]	59 ± 6	0.6905[a,†]	10
T-ag 110-135	0.7 ± 0.03	0.0001[a*,†]	55 ± 7	0.4503[a,†]	11
T-ag 110-135 + LMB	0.62 ± 0.03	0.1839[b,†]	47 ± 6	0.4509[b,†]	7
T-ag 110-135 + NCZ	0.68 ± 0.09	0.1509[b,‡]	57 ± 8	0.8914[b,†]	7

Rb, retinoblastoma protein; T-ag, SV40 large tumor antigen. Results expressed as mean ± SEM for the fractional recovery and half time of return of fluorescence ($t_{1/2}$).
[a]*P* values relative to GFP-Rb.
[b]*P* values relative to GFP-T-ag 110–135.
*Significant differences between the indicated samples.
†Student's *t*-test.
‡Mann–Whitney test.

110–135, including the NLS, but lacking all sequences responsible for conferring binding to DNA, Rb, p53 or Hsc/HSP70). Both GFP-Rb and GFP-T-ag are strongly enriched in the nucleus of transfected COS-7 cells, but to quite different extents (see Fig. 1A,B). Thus, to assess whether this relates in part to Rb's ability to bind to nuclear components such as the nuclear lamina [Markiewicz et al., 2002], we decided to use FRAP to compare the nucleocytoplasmic trafficking abilities of GFP fused to full-length Rb and the T-ag NLS. The results were quite distinct in terms of the fact that, in the case of GFP-Rb, the bleached area initially remained visible, whereas that for GFP-T-ag did not (see Fig. 2A, 0 s panels), consistent with differences between the two proteins in nuclear mobility/intranuclear binding. Quantitative analysis showed that the results for the recovery of nuclear fluorescence was significantly slower for GFP-Rb than for GFP-T-ag, with a $t_{1/2}$ of 70 s compared to 41 s, respectively (see Fig. 2A,C and Table I, see also Supplementary Materials, movies 1 and 2). The return of fluorescence in the photobleached area (fractional recovery of Fn) for GFP-Rb was just 0.46, in contrast to 0.89 for GFP-T-ag fusion protein; the latter value was closely comparable to that for GFP alone (0.91, $n = 5$), suggesting that GFP-T-ag does not associate with nuclear structures. To remove the influence of nucleocytoplasmic flux in the analysis, we also quantified the recovery of the nuclear to cytoplasmic ratio Fn/c (see Materials and Methods Section for details), with values of 0.45 and 0.94 for GFP-Rb and GFP-T-ag respectively (Fig. 2D), very similar to those obtained for the recovery of Fn. These results are consistent with the fact that Rb can bind to nuclear components [Templeton, 1992; Markiewicz et al., 2002], and a considerable portion (ca. 54%) of nuclear Rb remains immobile in the nucleus, whereas the T-ag construct containing only the NLS, lacks sequences conferring DNA binding, and is therefore comparatively more mobile. Comparison of the plots (Fig. 2B) for GFP-Rb and GFP-T-ag specific fluorescence of the nucleus (Fn) and cytoplasm (Fc) during the FRAP experiment demonstrated that T-ag cytoplasmic fluorescence decreases markedly with the return of nuclear fluorescence, whereas the changes for GFP-Rb are not so extensive.

RB IS HIGHLY IMMOBILE IN THE CYTOPLASM

Cytoplasmic bleaching was performed to analyze the nuclear export kinetics and mobility of GFP-Rb and GFP-T-ag fusion proteins. Initially, FRAP analysis of nuclear export was performed using GFP-Rb, which contains a CRM1-mediated NES [Jiao et al., 2006], and is known to bind cytoplasmic components such as tubulin and MTs in vivo [Roth et al., 2007]. Cytoplasmic bleaching results indicated that the rate of Rb nuclear export ($t_{1/2}$ of 62 s, Table I) is very similar to that for its nuclear import ($t_{1/2}$ of 70 s, Table I). Rb is also highly immobile in the cytoplasm, with a fractional recovery of only 0.41, implying that a considerable fraction of Rb protein remains bound/immobile in the cytoplasm, as it does in the nucleus (see Fig. 2A,C and Table I). Partial bleaching was observed in the cytoplasm, supporting this idea and consistent with the ability of Rb to bind MTs and tubulin in the cytoplasm [Roth et al., 2007] (see white boxes indicating the nonbleached residual fluorescence after bleaching, Fig. 3A). Only partial recovery after bleaching was observed as a result of diffusion from the cytoplasmic nonbleached residual fluorescence (see Fig. 3A,B). Results from FRAP performed in NCZ and LMB treated cells confirmed that Rb cytoplasmic recovery, was largely due to active nuclear export mediated by CRM1, as LMB treated cells showed a significantly slower rate of Rb cytoplasmic return ($t_{1/2}$ of 93 s, Fig. 3A,C and Table I), compared to untreated cells ($t_{1/2}$ of 62 s), but the fractional recovery was essentially the same (0.40 and 0.41). In contrast, in cells lacking functional MTs due to NCZ treatment, the fractional recovery of cytoplasmic fluorescence was significantly higher ($P < 0.05$) than in untreated cells (values of 0.51 and 0.41, respectively, Fig. 3A,C; see also Supplementary Material, movies 3–5), but no difference in the rate of recovery of cytoplasmic fluorescence was observed. This implies that MTs do not contribute to the Rb nuclear export process per se, but clearly have an effect on Rb's mobility (see Fig. 3A,B and Table I), as the Rb mobile fraction is significantly higher in cells lacking polymerized MTs.

Cytoplasmic bleaching experiments were also performed in cells expressing GFP-T-ag 110–135. In contrast to GFP-Rb, GFP-T-ag 110–135 showed significantly higher cytoplasmic mobility

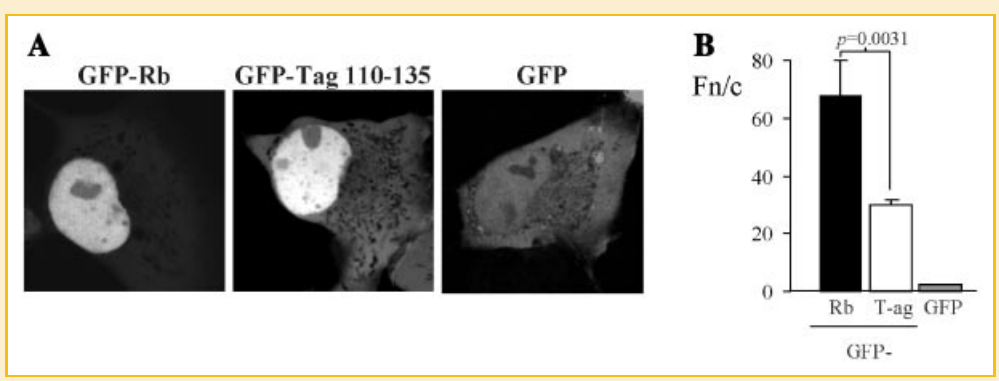

Fig. 1. GFP-Rb accumulates in the nucleus to a higher extent than GFP-T-ag 110–135. A: Confocal laser scanning microscopy (CLSM) images of transfected COS-7 cells expressing GFP-RB, GFP-T-ag 110–135 or GFP. B: Results for quantitative analysis of images such as those in (A) for the extent of nuclear accumulation of GFP-Rb, GFP-T-ag 110–135 or GFP, expressed as the Fn/c ratio [nuclear fluorescence (Fn) divided by the cytoplasmic fluorescence (Fc), after the subtraction of background fluorescence (Fb)]. Results represent the mean ± SEM ($n \geq 60$), where significant differences are denoted by *P* values.

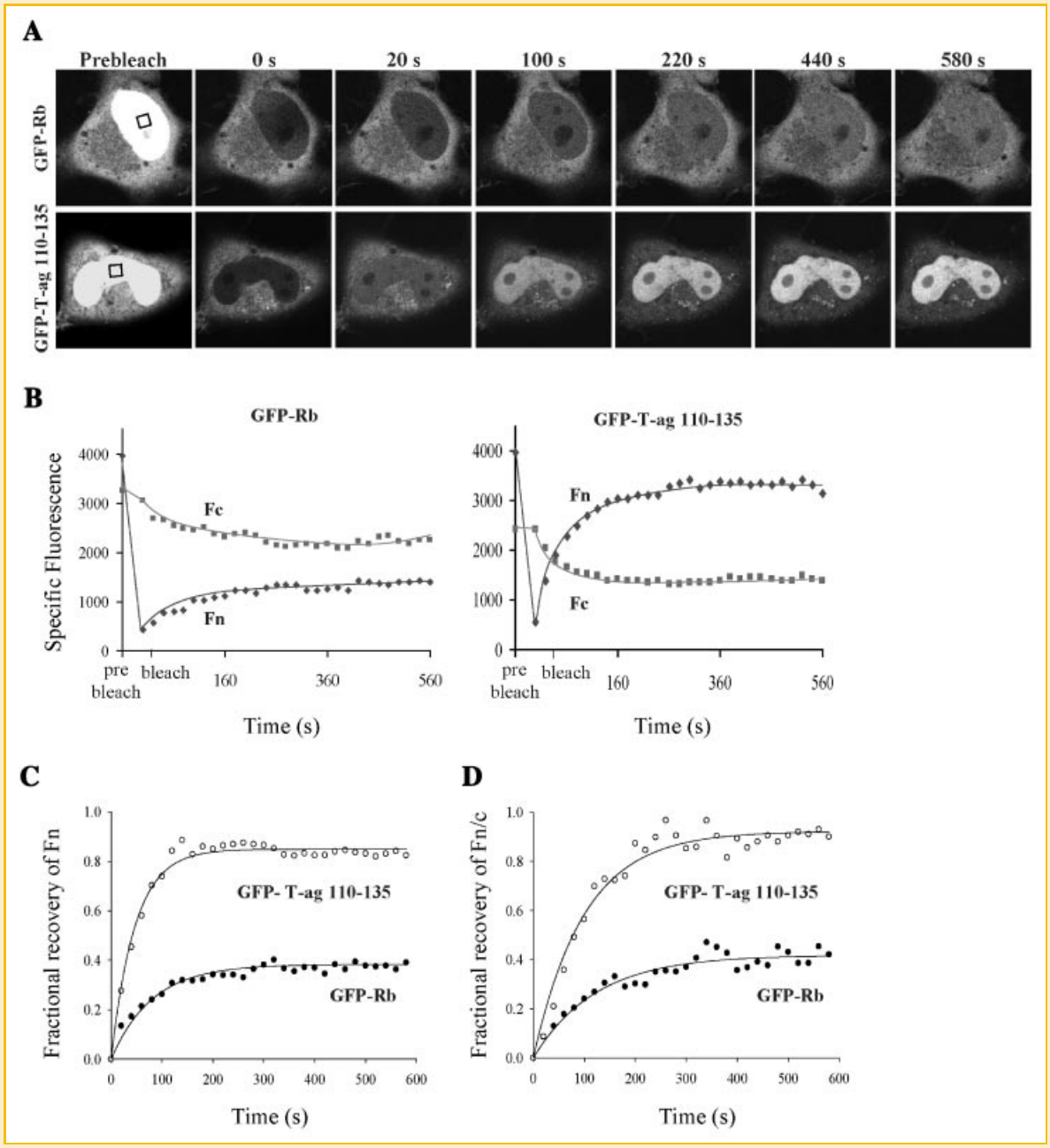

Fig. 2. Nuclear import of GFP–Rb is slower and shows a higher immobile fraction in the nucleus compared to GFP–T-ag 110–135. A: Visualization using CLSM of the return of nuclear fluorescence after photobleaching in transfected COS-7 cells expressing GFP–Rb or GFP–T-ag 110–135 (see Supplementary Material, movies 1 and 2). Black boxes indicate the bleached areas (~2 μm × 2 μm). B: Nuclear (Fn), and cytoplasmic (Fc) fluorescence after background subtraction was plotted against time. C: Quantification of the recovery over time of nuclear fluorescence after photobleaching expressed in terms of fractional recovery of Fn (Fn of respective time points divided by the prebleach Fn value), and corrected for the loss of fluorescence during the bleach and recovery periods (see Materials and Methods Section). D: Quantification of the recovery of Fn/c (Fn/c of respective time points divided by the prebleach Fn/c value).

($P = 0.0001$), with a mobile fraction of 0.7; no effect on cytoplasmic mobility was observed after either LMB or NCZ treatment. These results suggest that recovery of cytoplasmic fluorescence in the case of T-ag is due to free diffusion, as it does not contain an NES, and MTs do not affect cytoplasmic mobility of GFP-T-ag 110-135 (Fig. 3A,C). To rule out the possibility that cytoplasmic bleaching may damage the MT network, we fixed cells between 0 and 15 min after photobleaching, and immunostained for tubulin in order to visualise the MT filaments by CLSM. Cells analyzed at all times (Fig. 3D and not shown) showed clearly visible MTs in the bleached area indistinguishable from the MTs in the rest of the cell, as well as from those in adjacent non-bleached cells, consistent with the idea that the MT network is not affected by cytoplasmic bleaching using the conditions of this study.

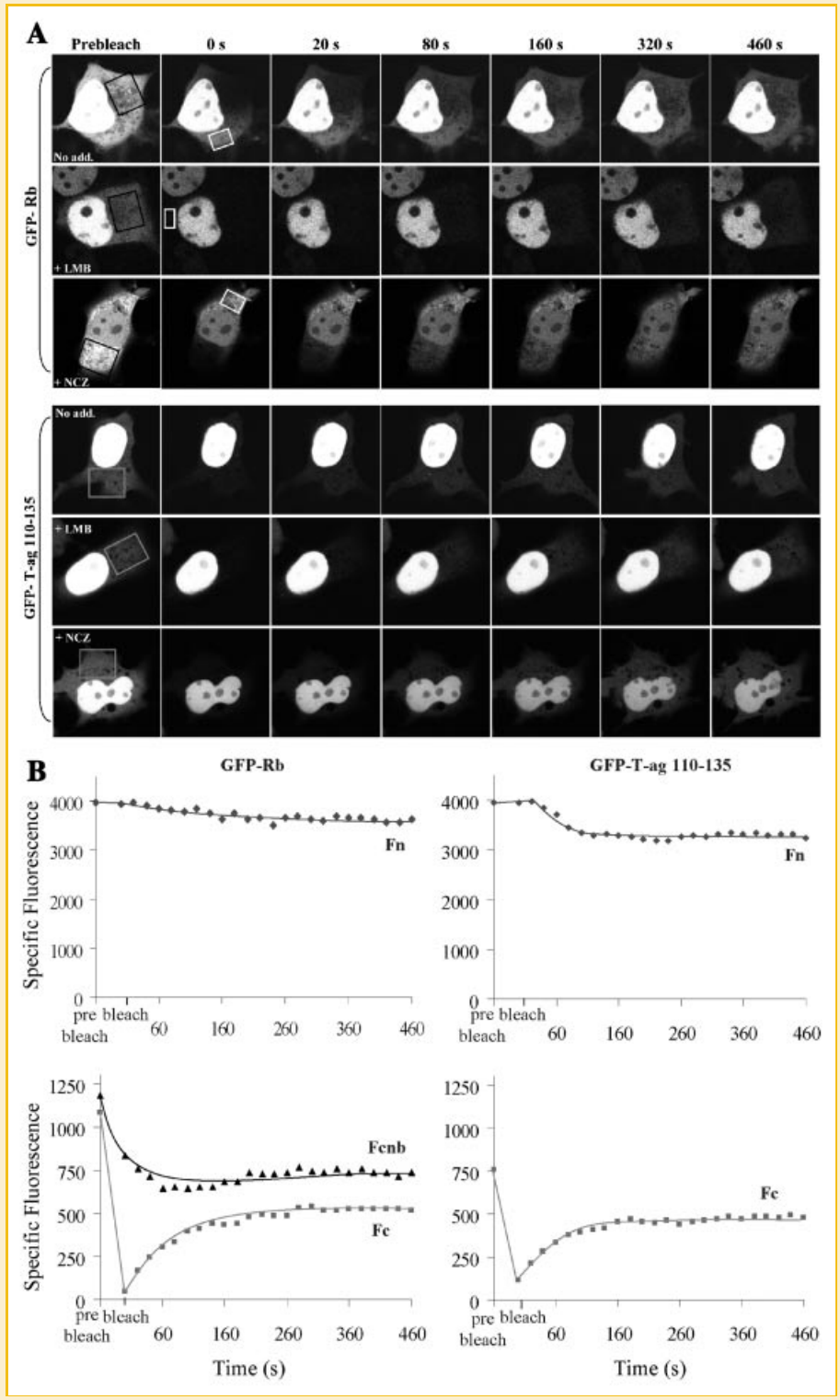

Fig. 3. GFP-Rb is highly immobile in the cytoplasm as opposed to GFP-T-ag 110–135. A: Visualization using CLSM of the return of cytoplasmic fluorescence after photobleaching in transfected COS-7 cells expressing GFP-Rb or GFP-T-ag 110–135 treated without or with NCZ or LMB (see Supplementary Material, movies 3–8). Black or gray boxes indicate the bleached areas ($\sim$12 μm $\times$ 12 μm), and white boxes the nonbleached cytoplasmic residual fluorescence. B: The nuclear (Fn), cytoplasmic (Fc), and the cytoplasmic nonbleached residual (Fcnb) fluorescence after background subtraction were plotted against time. C: Quantification of the recovery over time of cytoplasmic fluorescence after photobleaching expressed in terms of fractional recovery of Fc (Fc of respective time points divided by the prebleach Fc value), and corrected for the loss of fluorescence during the bleach and recovery period (see Materials and Methods Section). D: Visualization using CLSM of COS-7 cells expressing GFP-T-ag 110–135, with (1) or without (2) cytoplasmic bleaching using the typical FRAP protocol and immunostained for tubulin.

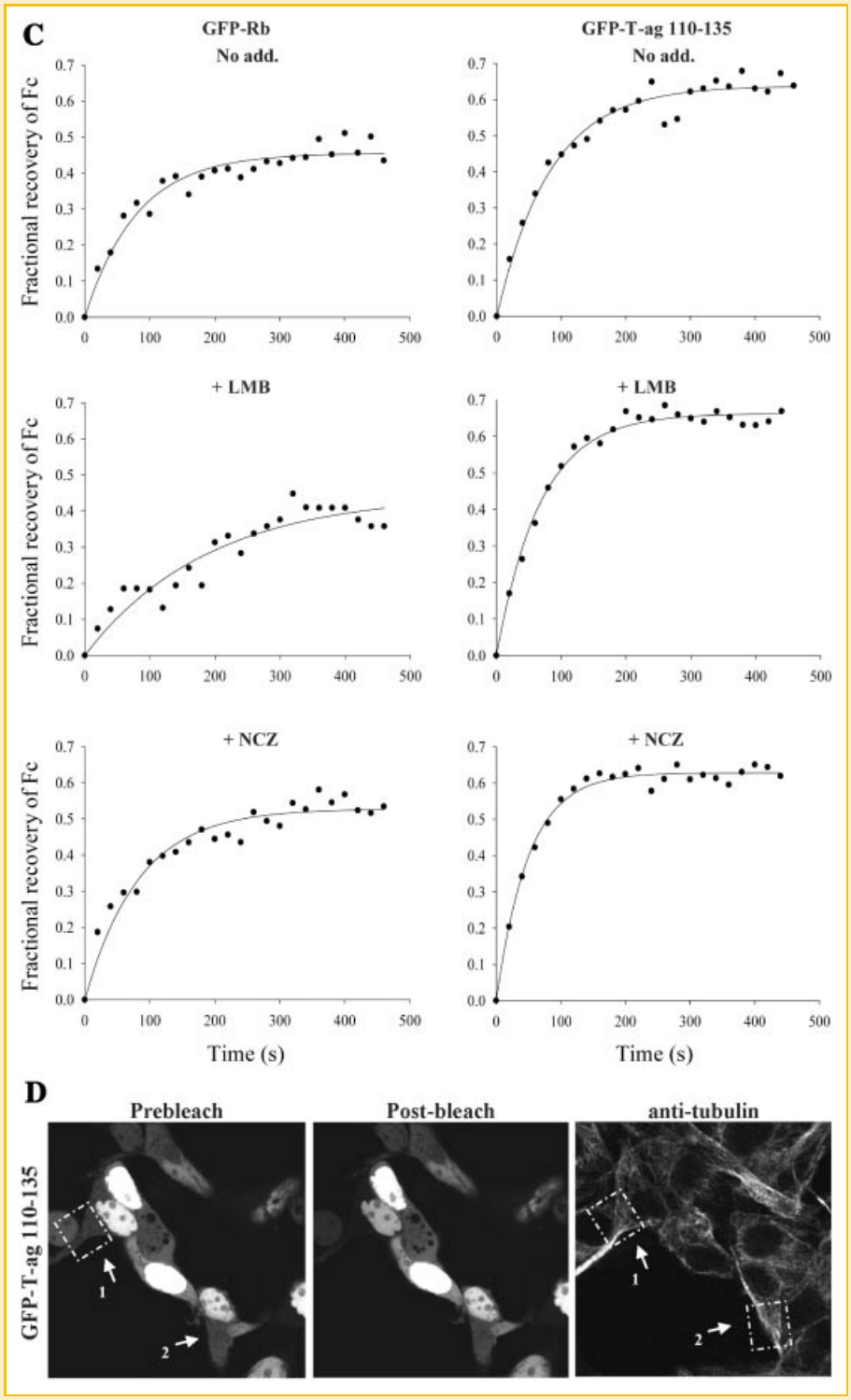

Fig. 3. (*Continued*)

Comparison of the plots for specific fluorescence of the nucleus (Fn), cytoplasm (Fc), and cytoplasmic nonbleached area (Fcnb) during the FRAP experiment (Fig. 3B), illustrate the differences between the two proteins, whereby the return of cytoplasmic fluorescence of GFP-Rb is partially a result of diffusion within the cytoplasm from the cytoplasmic nonbleached residual fluorescence (Fcnb), as well as from GFP-Rb nuclear export. In contrast, return of cytoplasmic fluorescence in cells expressing GFP-T-ag 110–135 results predominantly from nuclear T-ag diffusing into the cytoplasm, as bleaching in the cytoplasm is almost complete

without a visible residual nonbleached cytoplasmic area (Fcnb) (Fig. 3A,B; see also Supplementary Material).

DISCUSSION

FRAP was used here to analyze the nuclear import/export kinetics as well as intracellular mobility of two distinct NLS/NES-cargo proteins. FRAP has been previously used to analyze the mobility of nuclear binding proteins [Ellenberg and Lippincott-Schwartz, 1999; Kruhlak et al., 2000; Daigle et al., 2001; Kimura and Cook, 2001; Griffis et al., 2002; Carrero et al., 2003; Launholt et al., 2006], but very few studies have investigated the nuclear import and export of nuclear proteins [Lam et al., 2001, 2002; Nicolas et al., 2004; Schmierer and Hill, 2005; Sunn et al., 2005].

FRAP has an advantage over conventional in vitro nuclear transport assays in that cells are not physically damaged by microinjection, detergent, or mechanical perforation, meaning that cellular components important for trafficking, such as the MT network, are intact (see also Fig. 3D) [Giannakakou et al., 2000; Dohner et al., 2002]. Further, since the proteins are expressed intracellularly, their nucleocytoplasmic transport can be examined in as physiological a context as possible. Importantly, it allows the study of protein nuclear export kinetics, which is very difficult using in vitro techniques, since proteins first need to be introduced into the cell nucleus for nuclear export to be subsequently analyzed. Although FRAP has potential limitations of photodamage which can affect cellular proteins and structures, our experiments using bleach protocols as short as possible, clearly do not damage the MT network (see Fig. 3D) and, as previously shown [Lam et al., 2002], do not result in cytotoxicity. Here the settings were also optimized to bleach distinct parts of the cell, with experimental conditions for comparisons between different GFP-tagged proteins identical in all cases. GFP-tagged proteins were used in this study because GFP usually does not result in oxidative damage of neighboring molecules. The FRAP data was also normalized for loss of total fluorescence during the bleaching and recovery periods (see Materials and Methods Section) to yield more accurate results regarding protein mobility.

Here the nucleocytoplasmic trafficking and binding of the Rb protein in comparison with another nuclear localizing protein was demonstrated using FRAP for the first time. The results show that even though Rb and the T-ag NLS are imported into the nucleus by the same IMPα/β heterodimer dependent mechanism [Efthymiadis et al., 1997; Hubner et al., 1997], the kinetics of nuclear import and mobility differ markedly. Both GFP-Rb and GFP-T-ag fusion proteins accumulate in the nucleus with Fn/c ratios of ca. 70 and 30, respectively (Fig. 1A,B), indicating that their nuclear localization is mediated by the action of active transport as opposed to free diffusion (GFP has a Fn/c of ca. 1.5). T-ag nuclear import appeared to be significantly faster than that of Rb, consistent with previous in vitro studies comparing nuclear import mediated by the T-ag and Rb NLSs [Efthymiadis et al., 1997; Hu et al., 2005], attributed in part to the lower binding affinity of Rb to IMPα/β [Efthymiadis et al., 1997]. In contrast to the GFP-T-ag 110–135 construct, which lacks the DNA binding sequences of T-ag (amino acids 269–522) [VanLoock et al., 2002], a fraction of GFP-Rb remains immobile in the nucleus after photobleaching, consistent with its binding ability to nuclear components [Templeton, 1992; Markiewicz et al., 2002].

The cytoplasmic bleach experiments confirmed that Rb nuclear export is CRM1 dependent [Jiao et al., 2006], as LMB treatment significantly reduces its nuclear export rate. Interestingly, the rates of Rb nuclear import and nuclear export appear to be very similar, implying that other regulatory mechanisms may modulate Rb nucleocytoplasmic shuttling, for example, a large fraction of Rb also remains immobile in the cytoplasm partially due to association with the MT network, based on the increase of its mobile fraction after NCZ treatment (see Fig. 3).

In conclusion, FRAP has made possible to analyze the different nucleocytoplasmic trafficking and mobility of distinct nuclear proteins in living cells. In particular it was shown that Rb shuttles between nucleus and cytoplasm with similar rates, and is partially immobile in both, nucleus and cytoplasm cellular compartments, the latter in part due to Rb binding to the MT network. As Rb nuclear localization is essential for its tumor suppressor activity, better understanding of its trafficking mechanisms will provide important information for future studies with application in cancer development.

ACKNOWLEDGMENTS

The authors acknowledge the support of the National Health and Medical Research Council, Australia (fellowship #333013/#384109 and project grant #384107).

REFERENCES

Alvisi G, Jans DA, Guo J, Pinna LA, Ripalti A. 2005. A protein kinase CK2 site flanking the nuclear targeting signal enhances nuclear transport of human cytomegalovirus ppUL44. Traffic 6:1002–1013.

Carrero G, McDonald D, Crawford E, de Vries G, Hendzel MJ. 2003. Using FRAP and mathematical modeling to determine the in vivo kinetics of nuclear proteins. Methods 29:14–28.

Chan CK, Jans DA. 2002. Using nuclear targeting signals to enhance non-viral gene transfer. Immunol Cell Biol 80:119–130.

Daigle N, Beaudouin J, Hartnell L, Imreh G, Hallberg E, Lippincott-Schwartz J, Ellenberg J. 2001. Nuclear pore complexes form immobile networks and have a very low turnover in live mammalian cells. J Cell Biol 154:71–84.

Dohner K, Wolfstein A, Prank U, Echeverri C, Dujardin D, Vallee R, Sodeik B. 2002. Function of dynein and dynactin in herpes simplex virus capsid transport. Mol Biol Cell 13:2795–2809.

Efthymiadis A, Shao H, Hubner S, Jans DA. 1997. Kinetic characterization of the human retinoblastoma protein bipartite nuclear localization sequence (NLS) in vivo and in vitro. A comparison with the SV40 large T-antigen NLS. J Biol Chem 272:22134–22139.

Ellenberg J, Lippincott-Schwartz J. 1999. Dynamics and mobility of nuclear envelope proteins in interphase and mitotic cells revealed by green fluorescent protein chimeras. Methods 19:362–372.

Fornerod M, Ohno M, Yoshida M, Mattaj IW. 1997. CRM1 is an export receptor for leucine-rich nuclear export signals. Cell 90:1051–1060.

Forwood JK, Jans DA. 2002. Nuclear import pathway of the telomere elongation suppressor TR F1. inhibition by importin alpha. Biochemistry 41:9333–9340.

Ghildyal R, Ho A, Wagstaff KM, Dias MM, Barton CL, Jans P, Bardin P, Jans DA. 2005. Nuclear import of the respiratory syncytial virus matrix protein is mediated by importin beta1 independent of importin alpha. Biochemistry 44:12887–12895.

Giannakakou P, Sackett DL, Ward Y, Webster KR, Blagosklonny MV, Fojo T. 2000. p53 is associated with cellular microtubules and is transported to the nucleus by dynein. Nat Cell Biol 2:709–717.

Gorlich D, Kutay U. 1999. Transport between the cell nucleus and the cytoplasm. Annu Rev Cell Dev Biol 15:607–660.

Griffis ER, Altan N, Lippincott-Schwartz J, Powers MA. 2002. Nup98 is a mobile nucleoporin with transcription-dependent dynamics. Mol Biol Cell 13:1282–1297.

Harley VR, Layfield S, Mitchell CL, Forwood JK, John AP, Briggs LJ, McDowall SG, Jans DA. 2003. Defective importin beta recognition and nuclear import of the sex-determining factor SRY are associated with XY sex-reversing mutations. Proc Natl Acad Sci USA 100:7045–7050.

Henderson BR, Percipalle P. 1997. Interactions between HIV Rev and nuclear import and export factors: The Rev nuclear localisation signal mediates specific binding to human importin-beta. J Mol Biol 274:693–707.

Hu W, Kemp BE, Jans DA. 2005. Kinetic properties of nuclear transport conferred by the retinoblastoma (Rb) NLS. J Cell Biochem 95:782–793.

Hubner S, Xiao CY, Jans DA. 1997. The protein kinase CK2 site (Ser111/112) enhances recognition of the simian virus 40 large T-antigen nuclear localization sequence by importin. J Biol Chem 272:17191–17195.

Jans DA, Jans P. 1994. Negative charge at the casein kinase II site flanking the nuclear localization signal of the SV40 large T-antigen is mechanistically important for enhanced nuclear import. Oncogene 9:2961–2968.

Jans DA, Xiao CY, Lam MH. 2000. Nuclear targeting signal recognition: A key control point in nuclear transport? Bioessays 22:532–544.

Jiao W, Datta J, Lin HM, Dundr M, Rane SG. 2006. Nucleocytoplasmic shuttling of the retinoblastoma tumor suppressor protein via Cdk phosphorylation-dependent nuclear export. J Biol Chem 281:38098–38108.

Kimura H, Cook PR. 2001. Kinetics of core histones in living human cells: Little exchange of H3 and H4 and some rapid exchange of H2B. J Cell Biol 153:1341–1353.

Kruhlak MJ, Lever MA, Fischle W, Verdin E, Bazett-Jones DP, Hendzel MJ. 2000. Reduced mobility of the alternate splicing factor (ASF) through the nucleoplasm and steady state speckle compartments. J Cell Biol 150:41–51.

Lam MH, Briggs LJ, Hu W, Martin TJ, Gillespie MT, Jans DA. 1999. Importin beta recognizes parathyroid hormone-related protein with high affinity and mediates its nuclear import in the absence of importin alpha. J Biol Chem 274:7391–7398.

Lam MH, Henderson B, Gillespie MT, Jans DA. 2001. Dynamics of leptomycin B-sensitive nucleocytoplasmic flux of parathyroid hormone-related protein. Traffic 2:812–819.

Lam MH, Thomas RJ, Loveland KL, Schilders S, Gu M, Martin TJ, Gillespie MT, Jans DA. 2002. Nuclear transport of parathyroid hormone (PTH)-related protein is dependent on microtubules. Mol Endocrinol 16:390–401.

Launholt D, Merkle T, Houben A, Schulz A, Grasser KD. 2006. Arabidopsis chromatin-associated HMGA and HMGB use different nuclear targeting signals and display highly dynamic localization within the nucleus. Plant Cell 18:2904–2918.

Markiewicz E, Dechat T, Foisner R, Quinlan RA, Hutchison CJ. 2002. Lamin A/C binding protein LAP2alpha is required for nuclear anchorage of retinoblastoma protein. Mol Biol Cell 13:4401–4413.

Nicolas FJ, De Bosscher K, Schmierer B, Hill CS. 2004. Analysis of Smad nucleocytoplasmic shuttling in living cells. J Cell Sci 117:4113–4125.

Phair RD, Misteli T. 2000. High mobility of proteins in the mammalian cell nucleus. Nature 404:604–609.

Roth DM, Moseley GW, Glover D, Pouton CW, Jans DA. 2007. A microtubule-facilitated nuclear import pathway for cancer regulatory proteins. Traffic 8:673–686.

Schmierer B, Hill CS. 2005. Kinetic analysis of Smad nucleocytoplasmic shuttling reveals a mechanism for transforming growth factor beta-dependent nuclear accumulation of Smads. Mol Cell Biol 25:9845–9858.

Seydel U, Jans DA. 1996. Evidence for an inhibitory feedback loop regulating simian virus 40 large T-antigen fusion protein nuclear transport. Biochem J 315(Pt 1): 33–39.

Sunn KL, Eisman JA, Gardiner EM, Jans DA. 2005. FRAP analysis of nucleocytoplasmic dynamics of the vitamin D receptor splice variant VDR B1: Preferential targeting to nuclear speckles. Biochem J 388:509–514.

Templeton DJ. 1992. Nuclear binding of purified retinoblastoma gene product is determined by cell cycle-regulated phosphorylation. Mol Cell Biol 12:435–443.

VanLoock MS, Alexandrov A, Yu X, Cozzarelli NR, Egelman EH. 2002. SV40 large T antigen hexamer structure: Domain organization and DNA-induced conformational changes. Curr Biol 12:472–476.